

Kinetics of the Solid-State Phase Transformation of Form β to γ of Sulfanilamide Using Time-Resolved Energy-Dispersive X-ray Diffraction

Andrew K. Sheridan[†] and Jamshed Anwar*

Computational Pharmaceutical Sciences, Department of Pharmacy, King's College London, Manresa Road, London, U.K. SW3 6LX

Received July 28, 1995. Revised Manuscript Received January 30, 1996[⊗]

The kinetics of the solid-state phase transformation of form β to γ of sulfanilamide in powdered samples have been investigated using energy-dispersive X-ray diffraction (EDXRD) combined with synchrotron radiation. The β to γ transformation which is relatively fast has been followed in real time, courtesy of the high time resolution of the EDXRD method. The data obtained yield α -time curves of high accuracy and precision. The observed kinetics are atypical in that the transformation does not always proceed to completion but plateaus off, the rate and extent being higher with increasing temperature. This phenomenon suggests a distribution of activation energies in the powdered samples. Despite this complication the data have been analyzed by considering only the fraction transformed. Of the various kinetic models considered, the Avrami–Erofeyev ($n = 3.5$) and the Cardew model were found to best describe the data. The data fitting with both of these models, however, was not totally satisfactory. The Avrami–Erofeyev model was found to depart increasingly from the observed data at high α values. The Cardew model, being specific for powdered or polycrystalline samples, was significantly better, but only up to α values of about 0.85. Above this point the Cardew model deviates markedly from the observed data. Direct visual observation using hot-stage microscopy has revealed that the transformation always proceeds from a single nucleation event in each crystallite and that coalescence of growing surfaces and ingestion of potential nuclei are unimportant, which is consistent with the Cardew model. Also, extinction studies using polarized light have shown that the transformation in the crystallites is generally of the type single crystal to single crystal but does not exhibit any orientational relationship. The overall activation energy and the individual nucleation and growth activation energies for the β to γ transformation based on the Cardew model were determined to be 101 ± 7 , 142 ± 14 , and 70 ± 4 kJ/mol, respectively. The activation energy based on the Avrami–Erofeyev model was 89 ± 8 kJ/mol. These magnitudes are within the expected range for molecular crystals.

Introduction

Polymorphic phase transitions in crystals are of considerable scientific interest and industrial importance. The interest spans numerous fields that include Earth sciences,¹ materials science,² biomineralization,³ and explosives.⁴ The importance of phase transitions in crystals of pharmaceutical compounds is also well recognized, where unpredicted (and unwanted) phase transitions can adversely affect both the product activity and stability.⁵ In each of these disciplines a great deal of the interest is focused on the kinetics of the phase transitions involved. Thorough characterization of the

kinetics can enhance the fundamental understanding of the underlying molecular processes, assist in the rational design and development of materials and processes, and address uncertainties regarding the stability of the particular phases. Notable investigations of the kinetics of phase transitions include studies on metals and alloys,⁶ ceramics,⁷ inorganic compounds,⁸ and molecular crystals.⁹

The characterization of solid-state kinetics typically involves modeling the fraction transformed as a function of time (the α -time curve) on the basis of some topological mechanism. This form of characterization has been dominated by the kinetic model proposed (independently) by Avrami¹⁰ and Erofeyev,¹¹ which has found wide applicability. An important exception where the Avrami–Erofeyev model is inappropriate is, as demonstrated by the present study, the situation where the sample consists of a fine powder. Here the transformation resulting from any nucleation event is constrained to the individual crystallite by the crystallite's boundaries.

Modeling of the α -time curve is generally based on regression analysis. To be able to discriminate between the various kinetic models, it is essential that the data are of high quality and that the regression analysis is

[†] Present address: Zeneca Pharmaceuticals, Laboratory Complex, Hurdfield Industrial Estate, Macclesfield, Cheshire, SK10 2NA, UK.

* To whom correspondence should be addressed.

[⊗] Abstract published in *Advance ACS Abstracts*, March 15, 1996.

(1) (a) Matsui, M.; Price, G. D. *Nature* **1991**, *351*, 735–737. (b) Bassett, W. A.; Furnish, D.; Huang, E. *Solid-State Physics Under Pressure*; Minomura, S., Ed.; Terra Scientific Publishing Co.: 1985.

(2) (a) Andersson, C. A.; Gupta, T. K. *Adv. Ceram. 3 (Sci. Technol. Zirconia)* **1981**, 184–201. (b) Garvie, R. C.; Hannink, R. H.; Pascoe, R. T. *Nature* **1975**, *258*, 703–704.

(3) Bischoff, J. L.; Fyfe, W. S. *Am. J. Sci.* **1968**, *266*, 65–79.

(4) (a) Barton, A. F. M.; Hodder, A. P. W. *Chem. Rev.* **1973**, *73*, 127–139. (b) Karpowicz, R. J.; Sergio, S. T.; Brill, T. B. *I&EC Prod. Res. Dev.* **1983**, *22*, 363.

amply overdetermined. A variety of techniques have been used to monitor solid-state phase transformations as a function of time. These have included X-ray^{8a,b,17} and neutron¹² diffraction, differential scanning calorimetry,^{8c,e,9c} infrared spectroscopy,¹³ and dilatometry.¹⁴ In many investigations, typically the sample is removed from its test condition at the various time points, quenched, and then analyzed. This procedure can introduce error into the data as a change in the extent of transformation may occur during quenching and or analysis. Ideally data collection should be in situ and in real time, enabling the dynamic processes to be followed as they occur with the inherent accuracy.

Powder X-ray diffraction is ideal for studying solid-state polymorphic phase transformations, being both highly discriminatory between polymorphic forms¹⁵ and quantitatively accurate.¹⁶ Furthermore, as a result of advances in detector technology and the development of appropriate sample environments, the method now enables data to be collected in real time.^{12,17} A particularly important development is the energy-dispersive form of PXRD, EDXRD.¹⁸ In this technique a polychromatic "white" beam is used as the source of X-rays, and the diffraction data are collected at a fixed 2θ angle by an energy-dispersive detector. The detector discriminates between the photons to give an energy distribution of the photons at the fixed 2θ angle. The distinction between the conventional angle dispersive form of

powder X-ray diffraction (ADXRD) and EDXRD can be clearly conveyed by considering Bragg's law:

$$\lambda = 2d_{hkl} \sin \theta$$

where λ is the wavelength of radiation, d_{hkl} is the interplanar lattice spacing, and θ is the diffraction angle. In ADXRD λ is fixed and the reflections d_{hkl} are sampled by scanning 2θ , while in EDXRD θ is kept fixed and the reflections are sampled using radiation with a range of λ . The wavelength of a photon, λ , can be expressed in terms of its energy, E :

$$E = hc/\lambda$$

where h is Planck's constant and c is the speed of light in vacuum. Substituting this equation into Bragg's law yields

$$Ed_{hkl} \sin \theta = \text{constant}$$

which shows that for any fixed diffraction angle, θ , a range of interplanar lattice spacings, d_{hkl} , will cause diffraction of photons with discrete values of energy E .

The EDXRD technique is characterized by fast data collection since no scanning of the detector is involved and the whole diffraction pattern is recorded simultaneously. When combined with synchrotron radiation as a source of X-rays, the time resolution for this technique is typically of the order of 1 s, and with special refinements can be as low as 100 ms.¹⁹ The fixed 2θ angle is also useful in that it facilitates the design of environmental sample chambers (e.g., furnaces and pressure vessels) since only two small ports are required, one for the incident radiation and the other for the diffracted radiation. These characteristics make EDXRD an ideal technique for studying relatively fast solid-state phase transformations in real time.

This paper presents a time-resolved study of the thermal kinetics of a fast phase transformation in crystals of sulfanilamide (4-aminobenzenesulfonamide, $\text{NH}_2\text{C}_6\text{H}_4\text{SO}_2\text{NH}_2$) using EDXRD with synchrotron radiation. Sulfanilamide, an antibacterial drug, was selected as a model compound since its polymorphism is well characterized. It has been reported to exist in four polymorphic forms, and these are known to exhibit interesting phase transformations as a function of both temperature²⁰ and pressure.²¹ The thermodynamically stable form at room temperature is the β form. When heated above about 110 °C, it undergoes an irreversible first-order phase transformation to the γ . It is this transformation that has been investigated. (The term first order refers to the thermodynamic classification of the phase transformation according to Ehrenfest's²² scheme and not to the kinetic order of reaction.) The crystal data for the β ⁽²³⁾ and γ ⁽²⁴⁾ forms are listed in Table 1. The results from the present study suggest that the β - γ transformation is reconstructive. A cursory examination using molecular graphics did not reveal any easily recognizable geometrical relationship between the two crystal structures but only that they

(5) (a) Haleblain, J.; McCrone, W. *J. Pharm. Sci.* **1969**, *58*, 911–929. (b) Haleblain, J. *J. Pharm. Sci.* **1975**, *64*, 1269–1288. (c) Byrn, S. R. *Solid State Chemistry of Drugs*; Academic Press: New York, 1982. (d) *Pharm. J.* **1992**, Oct 10, 479.

(6) (a) Burgers, W. G.; Groen, L. *J. Discuss. Faraday Soc.* **1957**, *23*, 183–195. (b) Pati, S. R.; Cohen, M. *Acta Met.* **1969**, *17*, 189. (c) Raghavan, V.; Cohen, M. *Metall. Trans.* **1971**, *2*, 2409–2418. (d) Liu, Z.; Wang, G.; Zhang, Q. *J. Mater. Processing Technol.* **1994**, *44*, 75–80.

(7) (a) Whitney, E. D. *Trans. Faraday Soc.* **1965**, *61*, 1991–2000. (b) Villefuerte-Castrejon, M. E.; West, A. R. *J. Chem. Soc., Faraday Trans. 1* **1981**, *77*, 2297–2307.

(8) (a) Czanderna, A. W.; Rao, C. N. R.; Honig, J. M. *Trans. Faraday Soc.* **1958**, *54*, 1069–1073. (b) Rao, C. N. R. *Can. J. Chem.* **1961**, *39*, 498–500. (c) Barriga, C.; Morales, J.; Tirado, J. L. *J. Mater. Sci.* **1986**, *21*, 947–952. (d) Riedal, M.; Dassler, R. *J. Cryst. Growth* **1990**, *106*, 695–704. (e) Peric, J.; Krstulovic, R.; Feric, T.; Vucak, M. *Thermochim. Acta* **1992**, *207*, 245–254.

(9) (a) Kitaigorodskiy, A. I.; Mnyukh, Yu. V.; Asadov, Yu. G. *J. Phys. Chem. Solids* **1965**, *26*, 463–472. (b) Mnyukh, V. Yu. *Mol. Cryst. Liq. Cryst.* **1979**, *52*, 201–218. (c) Yokoyama, T.; Onishi, N.; Umeda, T.; Kuroda, T.; Kita, Y.; Kuroda, K.; Matsuda, Y. *Chem. Pharm. Bull.* **1986**, *34*, 917–921. (d) Richardson, M. F.; Yang, Q.; Novotny-Bregger, E.; Dunitz, J. D. *Acta Cryst. B: Struct. Sci.* **1990**, *B46* (5), 653–660.

(10) (a) Avrami, M. *J. Chem. Phys.* **1939**, *7*, 1103–1112. (b) Avrami, M. *J. Chem. Phys.* **1940**, *8*, 212–224. (c) Avrami, M. *J. Chem. Phys.* **1941**, *9*, 177–184.

(11) Erofeyev, B. V. *C. R. (Dokl.) Acad. Sci. URSS* **1946**, *52*, 511–514.

(12) Barnes, P.; Hausermann, D.; Tarling, S. E. *Inst. Phys. Conf. Ser. No. 111, Paper presented at the Int. Conf. on New Materials and their Applications*, University of Warwick, 1990; pp 61–66.

(13) Lennie, A. R.; Vaughan, D. J. *Am. Mineral.* **1992**, *77*, 1166–71.

(14) Viswanathan, U. K.; Kutty, T. R. G.; Ganguly, C. *Metall. Trans. A: Phys. Metall. Mater. Sci.* **1993**, *24*, 2653–2656.

(15) Anwar, J.; Tarling, S. E.; Barnes, P. *J. Pharm. Sci.* **1989**, *78*, 337–342.

(16) (a) Chung, F. *J. Appl. Crystallogr.* **1975**, *8*, 17–19 and references therein. (b) Hubbard, C. R.; Snyder, R. L. *Powder Diffraction* **1988**, *3*, 74–77. (c) Anwar, J. *J. Appl. Crystallogr.* **1993**, *26*, 413–421.

(17) (a) Gobel, H. E. *Adv. X-Ray Anal.* **1981**, *24*, 187–195. (b) Anwar, J.; Barnes, P. *Phase Transitions* **1992**, *39*, 3–11. (c) Engel, W.; Eisenreich, N.; Alonso, M.; Kolarik, V. *J. Thermal Anal.* **1993**, *40*, 1017–1024. (d) Forster, K. M.; Formica, J. P.; Richardson, J. T.; Luss, D. *J. Solid State Chem.* **1994**, *108*, 152–157.

(18) (a) Giessen, W. C.; Gordon, G. E. *Science* **1968**, *159*, 973–975. (b) Bordas, J.; Glazer, A. M.; Howard, C. J.; Bourdillon, A. J. *Phil. Mag.* **1977**, *35*, 311–323.

(19) Anwar, J.; Barnes, P.; Clark, S. M.; Dooryhee, E.; Häusermann, D.; Tarling, S. E. *J. Mater. Sci. Lett.* **1990**, *9*, 436–439.

(20) Lin, H. O.; Guillory, J. K. *J. Pharm. Sci.* **1970**, *59*, 972–975.

(21) (a) Junginger, H. *Pharm. Ind.* **1976**, *38*, 724–728. (b) Kala, H.; Traue, J.; Haack, U.; Moldenhaus, H.; Kedvessy, G.; Selmecki, B. *Pharmazie* **1982**, *37*, 674–675.

(22) Rao, C. N. R.; Rao, K. J. *Phase Transitions in Solids*; McGraw-Hill: New York, 1978.

Table 1. Crystallographic Data for the β and γ Polymorphs of Sulfanilamide

parameter	β form	γ form
a (Å)	8.975	7.95
b (Å)	9.005	12.945
c (Å)	10.039	7.79
β (deg)	111.43	106.50
Z	4	4
space group	$P2_1/c$	$P2_1/c$
density (g/cm ³)	1.514	1.486

differ in their hydrogen-bonding networks. The study clearly demonstrates both the high accuracy and the high time resolution attainable with EDXRD. Furthermore, it reveals the complex nature of the kinetics governing the β -to- γ transformation in powdered samples.

Experimental Section

β -Sulfanilamide. The commercial form of sulfanilamide (specified purity 99%+) obtained from Sigma was found to consist of the β form. The purity with respect to polymorphic form was verified using PXRD by comparison of the experimental diffraction pattern with a simulated one, generated from the single-crystal structure data²³ using the computer program Lazy Pulverix.²⁵ No contaminants were detectable. The chemical purity of the sample was determined using differential scanning calorimetry and found to be better than 99.9% w/w. Consequently the β -sulfanilamide was used as supplied without further purification or comminution. The sample was classified in terms of particle size by screening through a 50 μ m sieve, and the fraction below 50 μ m was used for the kinetic studies. The use of a such a particle size fraction is essential to minimize preferred orientation effects in powder diffraction studies. The single crystals used for hot-stage microscopy were prepared by recrystallization from acetone.

Energy-Dispersive X-ray Diffraction. The EDXRD experiments were carried out on the wiggler beamline 9.7 of the Synchrotron Radiation Source (SRS) at the SERC Daresbury Laboratory, Warrington, U.K. The SRS is a low-emittance storage ring that operates at 2GeV with a typical beam current of 200 mA. A description of the EDXRD setup on beamline 9.7 has been published by Clark.²⁶

The experimental geometry and the positions of the sample holder and heating stage are illustrated in Figure 1. Data were collected using transmission geometry with the diffraction angle fixed at $2.6^\circ 2\theta$. In transmission the volume of the sample contributing to the diffracted signal is that resulting from the intersection of the incident and diffracted beams, where the diffracted beam is defined by the fixed angle and the detector collimation. By adjusting the geometry of the experiment, the diffracting volume can be confined entirely within the sample, thereby excluding any diffraction signal from the aluminum sample holder from reaching the detector. The heating stage employed has been described by He et al.²⁷ It consists of a copper block at the center of which sits the sample enclosed in a thin aluminum tube. The block is heated by circulating oil. The temperature was controlled using a Eurotherm controller. The maximum rate of heating of the sample was limited to about 5 $^\circ$ C/min due to the large heat capacity of the oil bath. The latter, however, did ensure excellent temperature stability viz. $\pm 0.2^\circ$ C over 30 min. The maximum *controlled* rate of heating of the sample was considered to be too slow for achieving the desired isothermal

temperatures. Consequently, the heating stage was first equilibrated to the desired temperature and then the sample introduced. Preliminary experiments had shown that because of the large heat capacity of the cell the sample temperature would equilibrate rapidly within about 5–10 s. The sample consisted of approximately 500 mg of the β form of the drug. The temperature of the sample was determined using an in situ thermocouple embedded within the sample but out of the way of the incident beam. Diffraction patterns were collected every 10 s with a data collection time of 10 s/pattern.

Hot-Stage Microscopy. To complement the diffraction studies, the β -to- γ transformation was examined using a Nikon Microphot FXA optical microscope fitted with a hot stage. The specific aim was to generate direct visual data that could be used to verify the mechanism of transformation. The behavior of individual crystals of the β form during their transformation to the γ was recorded by a video camera attached to the microscope.

Results and Analysis

The time-resolved data obtained at 122.8 $^\circ$ C, typical of the data sets at other temperatures, is shown plotted in Figure 2. It clearly illustrates the time course of the transformation. As the transformation proceeds, the reflections of the β phase decline in intensity while those of the γ phase emerge and increase. At this temperature the transformation rate is very fast with the transformation going to completion within 6 min. Despite this, the high time resolution of the EDXRD technique is more than adequate for following the transformation; there are over 35 frames of data characterizing the 6 min transformation period.

The important parameter for kinetic analysis is the fractional transformation, α , as a function of time. To extract this from the EDXRD data, one needs to integrate the intensities under the individual reflections of the respective phases present in the sample. To achieve this, it is necessary either to have regions in the diffraction pattern where there is no overlap between the reflections or to decompose the pattern into individual contributions using entire-pattern profile fitting methods. Fortunately, for the present data, there are a number of nonoverlapping reflections that can be used directly for the determination of the fraction transformed.

For a *constant thickness* sample in which the volume of sample irradiated remains constant the mass fraction of any one phase is given by²⁸

$$I_j/I_0 = X_j \frac{\mu_j}{\mu_t}$$

where I_j/I_0 is the ratio of the relative integrated intensity of a selected reflection of one particular phase (phase j) in the mixture to its relative integrated intensity in the pure state; X_j is the mass fraction of the phase; and μ_j and μ_t are the mass absorption coefficients for the pure phase and the mixed sample, respectively. Since the mass absorption coefficients of two polymorphic forms of the same compound are identical, the ratio of the intensities yields the mass fraction directly.

The above theory is for the angle-dispersive form of PXRD employing the Bragg–Brentano reflection geom-

(23) O'Connell, A. M.; Maslen, E. N. *Acta Crystallogr.* **1967**, *22*, 134–145.

(24) Alleaume, P. M.; Decap, J. *Acta Crystallogr.* **1965**, *19*, 934–938.

(25) Yvon, K.; Jentschko, W.; Parthe, E. *J. Appl. Crystallogr.* **1977**, *10*, 73–74.

(26) (a) Clark, S. M. *Nuclear Instrum. Methods* **1989**, *A276*, 381.

(b) Clark, S. M. *Rev. Sci. Instrum.* **1992**, *63* (1), 863.

(27) He, H.; Barnes, P.; Munn, J.; Turrillas, X.; Klinowski, J. *Chem. Phys. Lett.* **1994**, *196*, 267.

(28) Klug, H. P.; Alexander, L. E. *X-ray Diffraction Procedures for Polycrystalline and Amorphous Materials*; Wiley: New York, 1974.

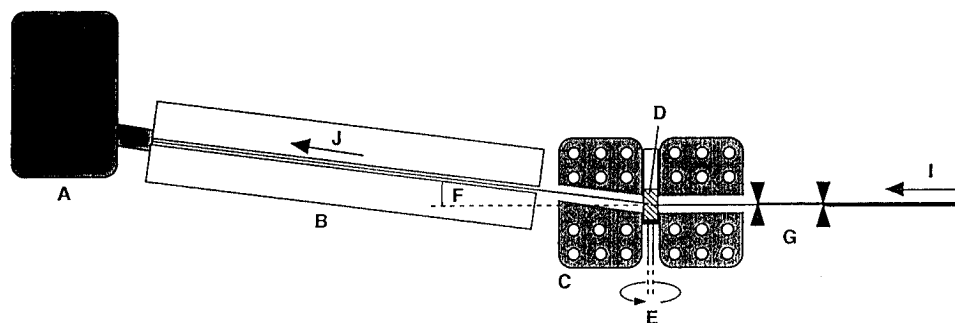


Figure 1. Energy-dispersive X-ray diffraction set up on beamline 9.7 at the SRS, SERC Daresbury Laboratory. (A) Solid-state energy-dispersive detector; (B) detector collimation system; (C) ceramic oil-filled heating block; (D) sample; (E) rotating sample holder; (F) fixed diffraction angle; (G) incident beam collimating system; (I) incident beam; (J) diffracted beam.

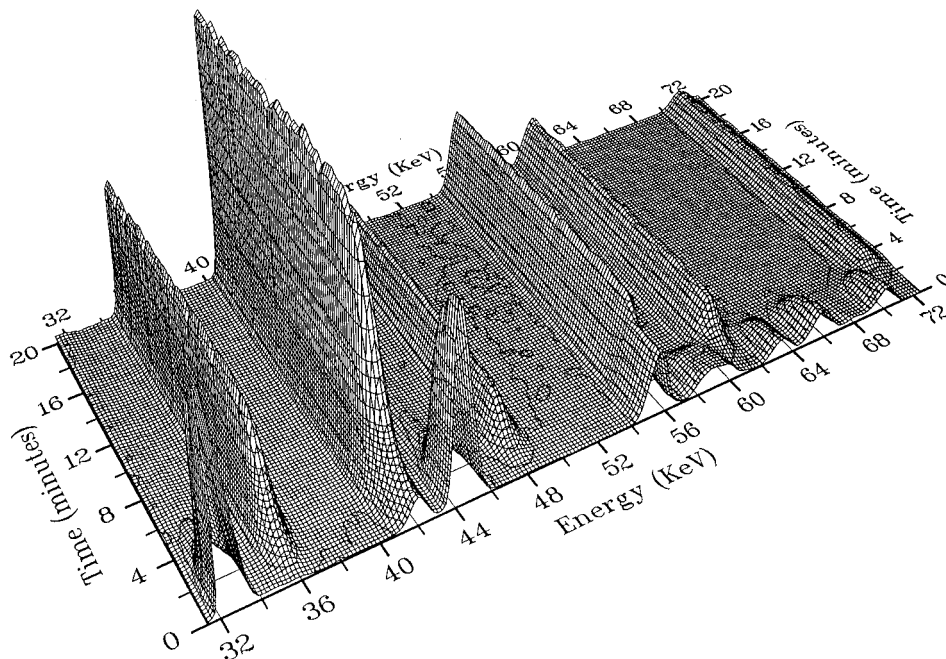


Figure 2. Time-resolved, energy-dispersive X-ray diffraction data for the β to γ transformation in sulfanilamide at 122.8 °C.

etry with fixed slits. It can also be applied to other forms of PXRD provided the volume of sample involved in diffraction remains constant. This is indeed the case for EDXRD since the diffraction angle remains fixed, which in turn keeps the diffracting volume fixed regardless of whether the geometry is transmission or reflection. Implicit in this assumption is that the bulk density of the sample remains constant throughout the transformation. In this respect we do expect some inaccuracy in the data reduction, since in the β -to- γ transformation there is about a 1.8% increase in volume and this may introduce some changes in the bulk packing of the sample during the transformation. An internal calibrant was not employed as it would have introduced significant peak overlap and complicated analysis.

The EDXRD patterns of the pure β and γ forms are shown in Figure 3. The significant reflections (100) and (110) of the β phase and (100), (110), and (011) of the γ phase were used in the determination of the mass fractions. The integrated reflection intensities were determined by means of profile fitting using the GENIE²⁹ suite of programs developed at the Rutherford Appleton Laboratory, Didcot, Oxon, UK. The integrated intensities were not normalized with respect to the decay in the incident beam flux as the decay was

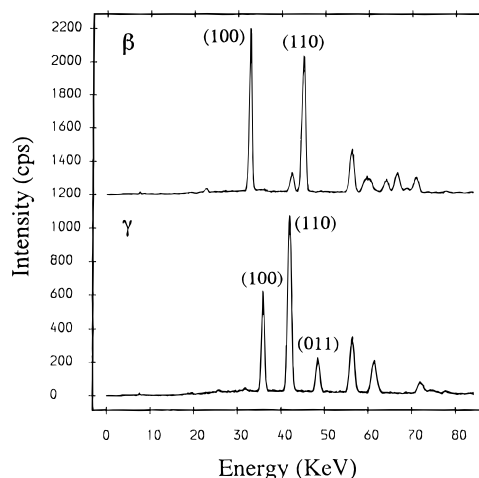


Figure 3. Energy-dispersive X-ray diffraction patterns of pure β and γ forms of sulfanilamide.

insignificant over the time frame of each kinetic experiment (typically 6–9 min).

The α -time curves for the transformation at each of the temperatures studied are shown in Figure 4. The

(29) David, W. F. I.; Johnson, M. W. K.; Knowles, J.; Morton-Smith, C. M.; Crosbie, G. D.; Campbell, S. P.; Lyall, J. S., Rutherford Appleton Laboratory publication no. RAL-86-102, 1986.

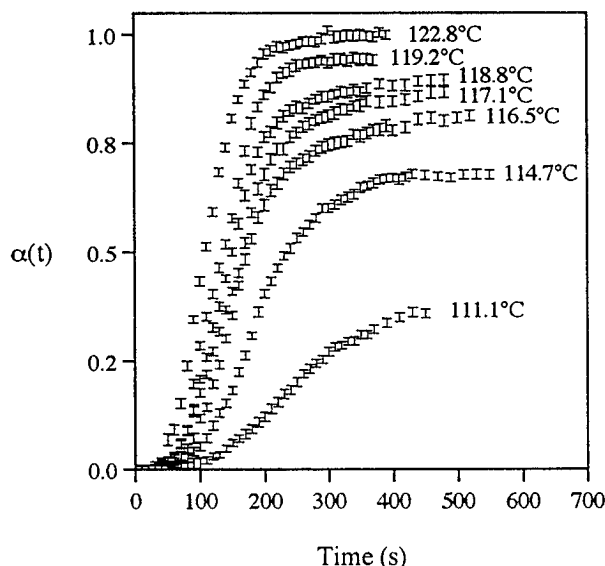


Figure 4. α -time curves for the β -to- γ transformation in sulfanilamide at various temperatures.

curves are sigmoidal in shape which is typical of many solid-state transformations in bulk powder samples. The time course of each of the curves is well characterized by many data points, courtesy of the high time resolution of the EDXRD technique. The precision of the data, as indicated by errors bars corresponding to $\pm\sigma$, is also very respectable. The standard deviations are the uncertainty in the profile fitting propagated through to α . In general, both the maximum extent of the transformation and the rate of transformation increase with increase in temperature. With the exception of the data collected at 122.8 °C the transformation fails to go to completion but rather plateaus off. Reasons for this are discussed later. A prerequisite however for kinetic analysis is that the reaction does proceed to completion. To overcome this problem, the data were rescaled to 100% converted so that for the purposes of analysis the transformation appears to go to completion. This is equivalent to ignoring any of the sample that remained untransformed. Consequently, any rate constant describing the transformation relates only to that portion of the sample that has actually transformed.

The rescaled data were tested for compatibility with a range of solid-state kinetic expressions using the computer program ISOKIN.³⁰ This program tests the experimental data against various kinetic models using least-squares analysis and provides a ranking of the fits. For all the data the Avrami–Erofeyev equation^{10,11} with an exponent of 3 or 4 ranked the highest, being the equation that most accurately described the data.

The Avrami–Erofeyev relationship assumes that the transformation proceeds by a nucleation-and-growth mechanism and takes into account the coalescence and ingestion of other nuclei as the new phase grows. Nucleation is assumed to be random, that is, if the entire sample was divided into small equal volumes, then the probability of a nucleus forming in each element in unit time is the same. The theory also assumes isotropic growth (equivalent growth rate in all

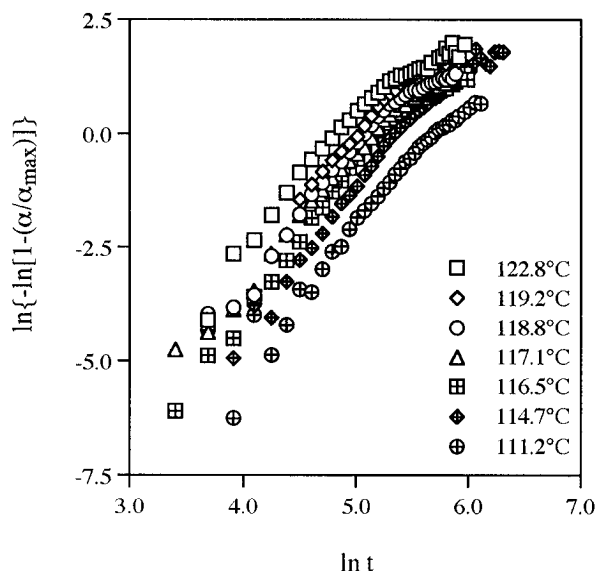


Figure 5. Determination of the Avrami–Erofeyev exponent n for the β -to- γ phase transformation in sulfanilamide. Due to the significant curvature exhibited by the data above α values of about 0.5, only the initial linear portions of each data set were used to determine the mean slope and hence a value of n .

three crystallographic directions) and that the number of potential nucleation sites are limited. The general relationship takes the form:

$$-\ln(1 - \alpha) = (kt)^n$$

where n can be

$$\begin{aligned} 3 \leq n \leq 4 & \quad \text{for three-dimensional growth} \\ 2 \leq n \leq 3 & \quad \text{for two-dimensional growth or} \\ 1 \leq n \leq 2 & \quad \text{for one-dimensional growth} \end{aligned}$$

The α -time data were analyzed using this equation, and the precise value of n was determined from a plot of $\ln[-\ln(1 - (\alpha/\alpha_{\max}))]$ vs $\ln t$ (shown in Figure 5) where α_{\max} is the maximum observed value of α for each data set. The exponent n is given by the gradient. The plots are linear up to an α value of approximately 0.5. Thereafter the transformation proceeds much more slowly than that predicted by the Avrami–Erofeyev relationship. This unpredicted retardation in the rate is discussed later. Using the linear portion of the data sets the mean value of the exponent n was determined to be 3.5 ± 0.1 . The rate constants were then estimated from plots of $-\ln(1 - (\alpha/\alpha_{\max}))^{1/3.5}$ vs time. These plots are shown in Figure 6.

Optical microscopy of the transformation revealed that only one nucleus appears to form in each crystallite and that this nucleus grows to engulf the entire crystallite without a second nucleus forming. A series of freeze frames showing this phenomenon in a typical crystallite is shown in Figure 7. The growth pattern from these single sites seems to possess a high degree of angularity that indicates that the moving interface might be following defined crystallographic directions. This prompted an investigation to ascertain whether an orientational relationship between the two phases (i.e., topotaxy) exists during the transformation. The respective parent and daughter phase extinction angles were

(30) ISOKIN, a program for modeling solid-state isothermal kinetic data (1989). Developed and distributed by J. Anwar, Department of Pharmacy, King's College London, Manresa Road, London SW3 6LX, U.K.

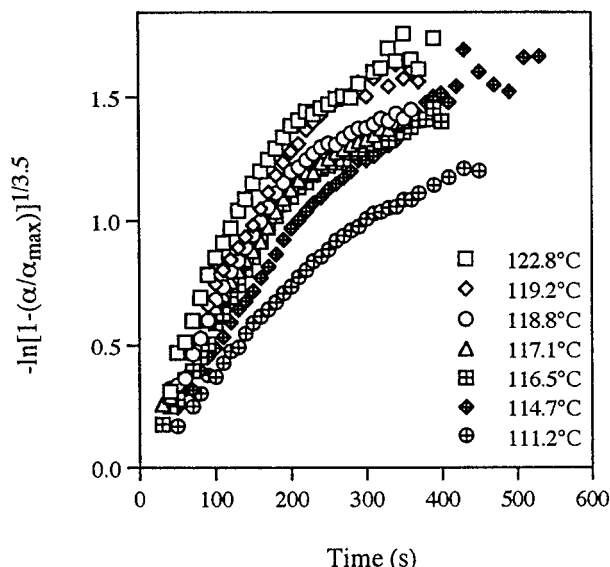


Figure 6. Avrami-Erofeyev plots for the β -to- γ transformation. Only the initial linear portions of the data sets ($\alpha < 0.5$) were used to determine the individual slopes and hence the rate constant for each temperature.

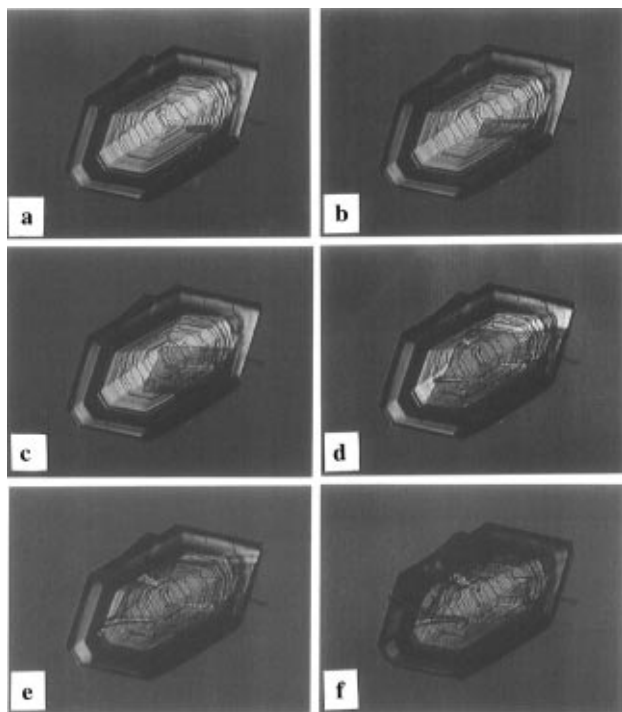


Figure 7. β -to- γ phase transformation in a single crystal of sulfanilamide at a temperature of 129 °C observed using a hot-stage microscope. The images show the γ phase initiating at a single nucleation site and then growing as a single crystal within the parent β crystal. The well defined interfaces bounding the crystal of the γ phase are clearly visible. The transformation was complete in just under 3 s. The crystal is about 1.7 mm in the longest dimension.

determined in 80 crystallites using crossed polarizers. The distribution of the angle defined by the parent and daughter extinction directions was observed to be random. These data indicate that the β -to- γ transformation is not characterized by a topotactic relationship.

The important conclusion from the microscopy is that the transformation in each crystallite proceeds from only a single nucleation site. The implication is that since coalescence of growing interfaces is not important, we

should expect departure from the Avrami-Erofeyev model at high values of α , which is indeed the case. In view of this, the data were tested using the alternative kinetic model of Cardew *et al.*³¹ The Cardew kinetic model describes the kinetics within the domain which lies between nucleation-controlled kinetics and the Avrami-Erofeyev model for which growth kinetics dominate. It was derived specifically for powdered or polycrystalline samples in which the transformation resulting from one nucleation event is constrained to a single crystallite within the sample. In such samples, provided the number of potential nucleation sites per crystallite are low, the coalescence and ingestion of nuclei by the growing phase characteristic of the Avrami-Erofeyev model are unimportant.

The Cardew model employs the ratio k_N/k_G to characterize the transformation behavior, where k_N and k_G are the nucleation and growth rate constants respectively. As this ratio tends to infinity, that is multiple nuclei occur within each crystallite, impingement of the growing nuclei becomes important and the overall kinetics follow the Avrami-Erofeyev model. As the ratio tends toward zero, the number of nucleation events per crystallite tends to unity, and the kinetics become nucleation controlled and follow the first-order kinetic model. The Cardew theory models the transformation behavior between these two extremes. The ratio k_N/k_G is sensitive to crystallite size; as the crystal size decreases the number of potential nucleation sites per crystal decrease hence causing the ratio to decrease. This dependence of the kinetics on crystallite size makes the Cardew model particularly suitable for powdered samples.

A key feature of the model is that it yields separate estimates of the rate constants k_N and k_G in contrast to the Avrami-Erofeyev model for which only a composite rate constant can be determined. The Cardew model takes the form

$$\alpha(t) = \frac{k_N}{k_G} \exp(-k_N t) \int_0^{k_G t} \exp\left(\frac{k_N}{k_G} u\right) \phi(u) du$$

where u is defined as $k_G t$, and ϕ is the fraction of crystallite that has transformed. For a random distribution of nucleation sites within the bulk of the crystal

$$\phi(u) = u^3(2 - u)^3$$

while for a random distribution of nucleation sites over the crystal surface

$$\phi(u) = u^2(2 - u)^2$$

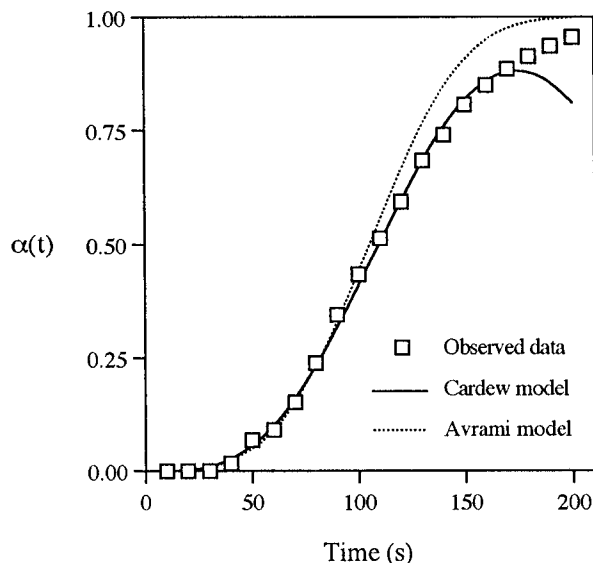
The rate constants k_N and k_G were estimated using the procedure outlined by Cardew *et al.* for each of the temperatures studied. The nucleation rate constant k_N was obtained from a plot of $-\ln[1 - (\alpha/\alpha_{\max})]$ vs time, being the slope of the exponential region. When this region is extrapolated to zero fraction converted, it intersects the time axis to give what Cardew *et al.* have termed the induction time for the transformation, τ_I . From a graphical estimate of τ_I it is possible to deter-

(31) Cardew, P. T.; Davey, R. J.; Ruddick, A. J. *J. Chem. Soc., Farad. Trans. 2* **1984**, *80*, 659-668.

Table 2. Kinetic Parameters for the β - γ Transition in Sulfanilamide Evaluated Using the Cardew Model

temp (°C)	τ_1 (s)	b^a	$1/k_N$ (s)	$1/k_G$ (s)	k_N/k_G	$f(a)$
122.8	97	0.670	35	145	4.14	0.79
119.2	113	0.674	39	168	4.31	0.80
118.8	115	0.648	51	177	3.47	0.74
117.1	122	0.645	56	189	3.38	0.73
116.5	129	0.647	59	199	3.37	0.73
114.7	147	0.633	77	232	3.01	0.70
111.2	162	0.606	125	267	2.14	0.59

^a b is equal to $\tau_1 k_G$ which is the slope of the plot $\{(k_N/k_G) + \ln[1 - f(a)]\}$ vs k_N/k_G .

**Figure 8.** Predicted Cardew and Avrami-Erofeyev α -time curves for the β -to- γ transformation in sulfanilamide at 122.8 °C superimposed on the observed data.

mine k_G through the following relationship:³¹

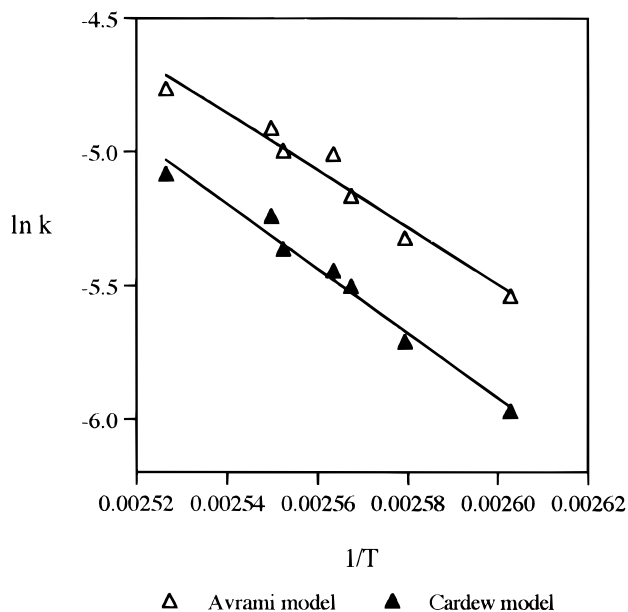
$$\tau_1 = \frac{1}{k_N} \left\{ \frac{k_N}{k_G} + \ln[1 - f(a)] \right\}$$

where $f(a)$ is the fraction converted at time $t = 1/k_G$ and is given by

$$f(a) = \frac{k_N}{k_G} \exp\left(-\frac{k_N}{k_G}\right) \int_0^1 \exp\left(\frac{k_N}{k_G} u\right) \phi(u) du$$

From a plot of $\{(k_N/k_G) + \ln[1 - f(a)]\}$ vs k_N/k_G a value for k_G can be obtained. The time constants evaluated from such an analysis are listed in Table 2. The k_G and k_N values were used in the Cardew equation to generate a predicted α -time curve. The predicted Cardew and Avrami-Erofeyev curves are shown plotted alongside the observed data for the 122.8 °C experiment in Figure 8. The consistency between the observed data and the Cardew model, which is typical of data sets at other temperatures, is very good up to α values of about 0.85. In this range the Cardew model is significantly better than the Avrami-Erofeyev model. At higher values of α , however, the Cardew model deviates markedly from the observed data.

Since the Avrami-Erofeyev model describes the data with a high degree of precision up to values of approximately 0.5, it was decided to use the rate constants obtained by this analysis to construct an Arrhenius plot. To compare the data treated in this fashion with that obtained from the Cardew kinetic model, the individual

**Figure 9.** Arrhenius plots for the β -to- γ transformation in sulfanilamide using rate constants determined from the Avrami-Erofeyev analysis and the Cardew analysis.**Table 3. Rate Constants for the β - γ Transition in Sulfanilamide**

temp (°C)	k (Avrami) ($\times 10^{-3} \text{ s}^{-1}$)	K' (Cardew) ($\times 10^{-3} \text{ s}^{-1}$)	k_N ($\times 10^{-2} \text{ s}^{-1}$)	k_G ($\times 10^{-3} \text{ s}^{-1}$)
122.8	8.548	6.198	2.857	6.897
119.2	7.353	5.297	2.464	5.952
118.8	6.757	4.691	1.961	5.650
117.1	6.667	4.318	1.786	5.291
116.5	5.714	4.070	1.695	5.025
114.7	4.884	3.307	1.299	4.310
111.2	3.929	2.553	0.800	3.745

Cardew rate constants for growth (k_G) and nucleation (k_N) were reduced to an overall rate constant (K'). This was achieved through the following relationship taken from Cardew et al.:³¹

$$K' = \left[\frac{2}{k_N} \left(\frac{1}{k_G} \right)^3 \right]^{1/3.5}$$

The rate constants are tabulated in Table 3. The respective Arrhenius plots for both models are shown in Figure 9. Both plots are linear, the correlation coefficients being 0.960 and 0.978 for the Avrami-Erofeyev model and the Cardew model, respectively.

Arrhenius plots were also constructed for both the nucleation and growth rate constants (obtained using the Cardew model) and are shown in Figure 10. The corresponding activation energies and preexponential frequency factors characterizing the two processes are listed in Table 4.

Discussion

A sigmoidal α -time curve is typical of many solid-state phase transformations regardless of the underlying topological mechanism. Consequently it can be difficult to distinguish between the various kinetic models purely on the basis of modeling the α -time data. This problem is compounded when trying to analyse curves based on relatively few data points and where each determination is imprecise. The need for high-quality, high-precision quantitative data is paramount. The α -time curves shown in Figure 4 clearly illustrate the high quality of

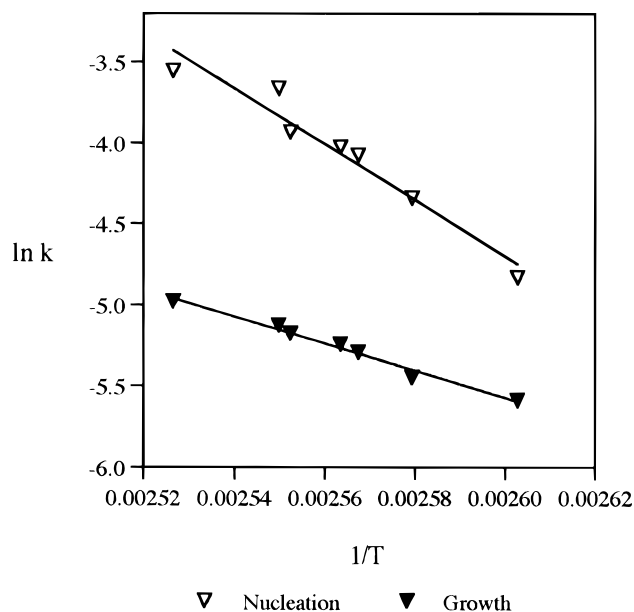


Figure 10. Arrhenius plots for the β -to- γ transformation in sulfanilamide using the separate nucleation and growth rate constants determined from the Cardew analysis.

Table 4. Thermodynamic Data for the β - γ Transition in Sulfanilamide

kinetic model	E^{\ddagger} (kJ mol ⁻¹)	Arrhenius constant (s ⁻¹)
Cardew et al.	101 ± 7	1.3 × 10 ¹¹
Avrami-Erofeyev	89 ± 8	4.6 × 10 ⁹
Cardew et al.		
nucleation	142 ± 14	2.0 × 10 ¹⁷
growth	70 ± 4	1.1 × 10 ⁸

data obtained using the real-time EDXRD technique. Each curve is well characterized with a large number of data points and each data point is known to a high precision ($\sigma(\alpha) < 0.015$).

The β -to- γ transformation in sulfanilamide as observed microscopically in single crystals proceeds via a single nucleus. The nucleus of the γ phase grows with defined interfaces until the crystal is entirely transformed. Extinction studies reveal that in general the transformation is of the type single crystal to single crystal. This is rather uncommon in molecular crystals and requires that the increase in volume associated with the transformation (about $1.8 \pm 0.5\%$ for β to γ) is accommodated in some specific manner. More commonly the stress induced by the change in volume causes a massive disruption of the crystal resulting in a polycrystalline sample, with the crystal either cracking but retaining its overall morphology or fragmenting. As to how the strain might be relieved for the β -to- γ transformation without disrupting the crystal may be inferred from the electron micrograph of the transformed crystal in Figure 11. The surface of the transformed crystal shows regular corrugation, indicative of counter-slippage of lattice planes which maintain the coherency of the lattice and at the same time accommodate the volume change. The extinction studies also reveal that the lattices of the two phases do not exhibit any specific orientational relationship (i.e., topotaxy) during the transformation. The implication is that there is no one defined molecular pathway for this transformation.

The α -time curves shown in Figure 4 clearly reveal the complex nature of the kinetics governing the β -to- γ

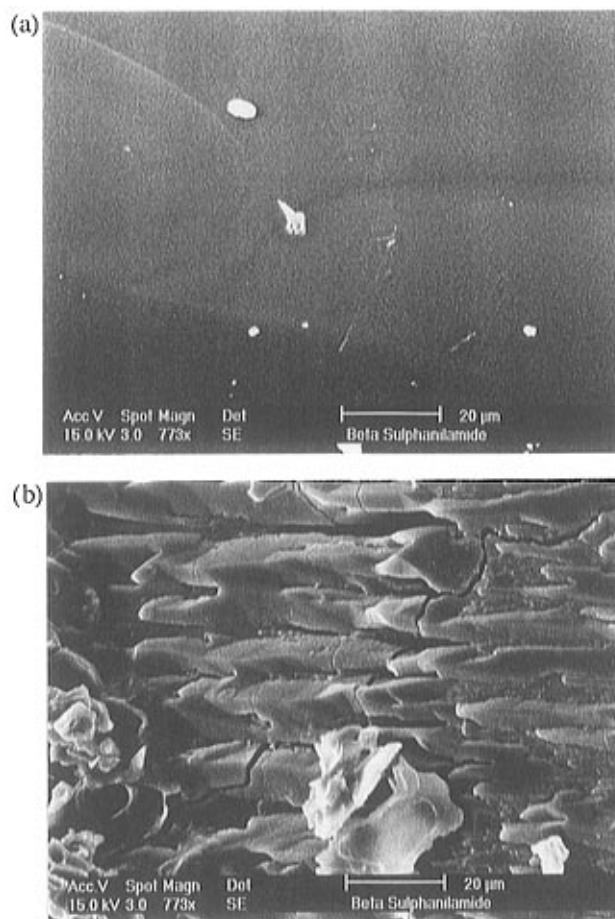


Figure 11. Electron micrographs of a single crystal of sulfanilamide before (a) and after (b) undergoing a transformation from the β to the γ form. The corrugated appearance of the surface of the γ form suggests widespread slippage of lattice planes during the transformation.

transformation. With the exception of the 122.8 °C dataset, the transformation fails to go to completion and plateaus off within the time scale of the experiment. Not only is the rate of transformation influenced by temperature but also the extent to which it proceeds, the maximum extent of transformation being greater at higher temperatures. This behavior is not common but appears to be a characteristic of phase transitions in polycrystalline or powdered samples.^{17b,32} It can be explained in physical terms using Magee's^{32b} ideas. The nucleation sites, being sites of lattice defects and imperfections, are characterized by a distribution of activation energies. In a powdered sample these sites will be randomly distributed throughout the crystallite population. Consequently, at any given temperature only those crystallites that contain nuclei for which the probability of activation is significant will transform. All others will remain untransformed. At higher temperatures, crystallites containing sites with higher activation energies become involved, thereby increasing the overall extent of the transformation. In contrast, transformations in samples consisting of larger crystals almost invariably go to completion. Here, although there is still a distribution of activation energies characterising the defects, only the minimum activation

(32) (a) Cech, R. E.; Turnbull, D. *AIME Trans.* **1956**, *206*, 124–132. (b) Magee, C. L. *Metall. Trans.* **1971**, *2*, 2419–2430. (c) Raghaven, V.; Cohen, M. *Metall. Trans.* **1971**, *2*, 2409–2418.

energy, E_{\min}^{\ddagger} , is important. If each crystal is large enough to contain at least one site characterized by E_{\min}^{\ddagger} , then the nucleation of each of these sites is sufficient to cause transformation of each crystal and hence the whole sample. Sites of higher activation energy become consumed during the transformation and therefore remain unimportant.

A framework of kinetic analysis that attempts to include the refinement of a distribution of activation energies has been proposed by Magee.^{32b} This procedure, however, includes additional parameters that are unknown for the β -to- γ transformation. Conventional kinetic analysis requires that the transformation proceeds to completion. To progress from this complication, the data for each temperature have been normalized with respect to the maximum extent of transformation, α_{\max} . In physical terms this means that any of the sample which remains untransformed is ignored. Consequently, the rate constant(s) for each isothermal temperature will be characteristic only for the portion of sample that transformed at that temperature and not the whole sample. This will also be reflected in the mean activation energy characterizing each of the different portions of sample; the mean activation energy will be greater for a portion of sample transformed at a higher temperature, since crystallites that would have remained unreacted at a lower temperature now also become involved. There is, of course, some overlap since the fraction transformed at any lower temperature is a subset of the fraction transformed at any higher temperature. The expectation from these considerations is that the mean activation energy, determined using the procedure outlined, should show a continuous increase with increase in temperature. In many instances, however, this expected increase in mean activation energy may be offset by what is termed the *compensation effect*.³³ This phenomenon arises due to the thermal expansion of the lattice which tends to reduce the activation energy for nucleation by increasing steric freedom. How these two opposing effects affect the shape of the Arrhenius plot will depend on the substance being studied. The Arrhenius plots for the β -to- γ transformation do not enable any categorical conclusions to be drawn in this respect.

The Avrami–Erofeyev equation was developed specifically to describe the kinetics of solid-state phase transformations. Indeed, it ranks topmost in modeling the β -to- γ transformation data using regression analysis. Despite this success, there is significant departure between the observed data and the Avrami–Erofeyev model at $\alpha > 0.5$. In comparison the Cardew model, which was derived specifically for powdered samples where growth becomes restricted by crystallite boundaries, gives very good agreement with the observed data but only up to α values of about 0.85 (see Figure 8). Above this the Cardew model goes through a maximum and then sharply drops toward the time axis. Closer analysis of the Cardew function has revealed that this behavior is characteristic of this model and does not imply that the present data are outside the legitimate scope of this function. It is therefore clear that the current analytical functions are not wholly adequate for

modeling the complex kinetics observed. An alternative approach, albeit not as elegant as an analytical solution, is to employ numerical simulation. This approach is feasible since the topological processes involved in phase transitions of a polycrystalline samples are well understood. Such an approach should also enable the incorporation of a distribution of activation energies.

The activation energies and preexponential factors for the β -to- γ transformation determined from both the Avrami–Erofeyev and the Cardew analysis (with a composite rate constant) are listed in Table 4. Considering the heterogeneous nature of solid-state phase transformations, the activation energies from the two procedures, 89 ± 8 kJ/mol (Avrami–Erofeyev) and 101 ± 7 kJ/mol (Cardew) are not considered to be significantly different. This is expected as both kinetic models are based on a mechanism of nucleation and growth and the Cardew model is a refinement of the Avrami–Erofeyev model. The magnitude of the activation energy is within the expected range for molecular crystals, namely, 100–200 kJ/mol.³³ The preexponential frequency factor in a solid-state transformation is commonly reconciled with the lattice vibration frequency which is of the order of 10^{13} s⁻¹. This value is usually taken to be a good check on thermal kinetic analysis. Estimates that differ markedly from this value are indicative of complications. The values of 10^9 s⁻¹ (Avrami) and 10^{11} s⁻¹ (Cardew) for the present analysis are respectable.

The fundamental parameters characterizing the kinetics are the activation energies E_N^{\ddagger} and E_G^{\ddagger} for the nucleation and growth processes, respectively. Associated with these parameters are the rate constants k_N and k_G . In general, it is not possible to estimate the individual parameters from an α -time curve, and one can only extract an overall rate constant. Indeed this is the case with the usual form of the Avrami–Erofeyev model. The Cardew model, on the other hand can under certain circumstances enable the estimation of both the rate constants. This depends on the ratio of the rate constants. When this ratio is away from the two extremes of zero (nucleation-controlled kinetics) and infinity (Avrami–Erofeyev kinetics) then both constants can be determined. The ratio k_N/k_G for the β -to- γ transformation is on average about 3.4, thus enabling the individual rate constants to be estimated. The corresponding estimates for the activation energies are 142 ± 14 and 70 ± 4 kJ/mol for the nucleation and growth processes, respectively. This suggests that the transformation is dominated by nucleation. This would seem reasonable as nucleation is clearly the limiting step for the portion of sample that remains untransformed at any given temperature.

In summary, energy-dispersive X-ray diffraction is a powerful real-time technique that has been shown to be ideal for the study of rapid phase transformations. It yields accurate data and has been successfully employed to characterize the β -to- γ polymorphic phase transformation in the drug sulfanilamide. The kinetics of the transformation are complex and suggest that the powdered samples may be characterized by a distribution of activation energies rather than a single value. Despite this, analysis of the kinetic data has been attempted using the kinetic models of Avrami–Erofeyev and Cardew et al. The Cardew model, which is specific

(33) Brown, W. E.; Dollimore, D.; Galway, A. K. *Reactions in the Solid State*, Bamford, C., Tipper, C., Eds.; Elsevier Scientific Publishing Co.: Amsterdam, 1980; Vol. 22 of *Comprehensive Chemical Kinetics*.

for a polycrystalline sample and thus the most appropriate for the present samples, was found to best describe the data, albeit not totally satisfactory. Additional microscopic evidence supports the use of this model. Finally it is clear from the study that although the possible topological mechanisms are conceptually well understood, the current analytical kinetic models (including the Avrami–Erofeyev and the Cardew models) are not wholly adequate in describing the complex kinetics observed.

Acknowledgment. We would like to thank Simon Clark of the SRS, SERC Daresbury Laboratory, and

Paul Barnes, Department of Crystallography, Birkbeck College London, for their advice and assistance in using the X-ray diffraction facility on Station 9.7 of the SRS; Xavier Turrallis, Birkbeck College London, for producing the 3-D plot in Figure 2; and also Dave McCarthy, School of Pharmacy London, for use of the microscope and image-processing facilities. We also wish to acknowledge the SERC for the funding of a Ph.D. studentship (A.K.S.) and the beam-time allocation. Finally, we are grateful to Peter Cardew, NWW Acumen Ltd., for useful discussions and for reviewing the manuscript.

CM950349Z